Tuomisto, Filip; Karjalainen, Antti; Makkonen, Ilja

Split Ga vacancies

Published in:
Oxide-Based Materials and Devices XII

DOI:
10.1117/12.2585462

Published: 01/01/2021

Document Version
Publisher's PDF, also known as Version of record

Please cite the original version:
Tuomisto, F., Karjalainen, A., & Makkonen, I. (2021). Split Ga vacancies: Abundant defects in β-Ga_2O_3. In D. J. Rogers, D. C. Look, & F. H. Teherani (Eds.), *Oxide-Based Materials and Devices XII* Article 2585462 (Proceedings of SPIE - The International Society for Optical Engineering; Vol. 11687). SPIE. https://doi.org/10.1117/12.2585462

PROCEEDINGS OF SPIE

SPIEDigitalLibrary.org/conference-proceedings-of-spie

Split Ga vacancies: abundant defects in beta-Ga2O3

Tuomisto, Filip, Karjalainen, Antti, Makkonen, Ilja

Filip Tuomisto, Antti Karjalainen, Ilja Makkonen, "Split Ga vacancies: abundant defects in beta-Ga2O3," Proc. SPIE 11687, Oxide-based Materials and Devices XII, 1168709 (5 March 2021); doi: 10.1117/12.2585462

SPIE.

Event: SPIE OPTO, 2021, Online Only

Split Ga vacancies: abundant defects in β-Ga_2O_3

Filip Tuomisto*[a], Antti Karjalainen[a,b], Ilja Makkonen[a]
[a]Department of Physics and Helsinki Institute of Physics, University of Helsinki, P. O. Box 43, FI-00014 Helsinki, Finland
[b]Department of Applied Physics, Aalto University, POB 15100, FI-00076 Aalto Espoo, Finland

ABSTRACT

We have applied positron annihilation spectroscopy to study a wide range of β-Ga_2O_3 bulk crystals and thin films with various doping levels. The Doppler broadening of the 511 keV positron-electron annihilation line exhibits colossal anisotropy compared to other three-dimensional crystalline semiconductors. State-of-the-art theoretical calculations of the positron characteristics in the β-Ga_2O_3 lattice reveal that the positron state is effectively 1-dimensional, giving rise to strong anisotropy. Strongly relaxed split Ga vacancies are found to exhibit even stronger anisotropy and to dominate the positron annihilation signals in almost all experiments. The evidence leads to the conclusion that split Ga vacancies are abundant, with concentration of 10^{18} cm^{-3} or more, in β-Ga_2O_3 samples irrespective of conductivity.

Keywords: positron annihilation spectroscopy, gallium oxide, defect, vacancy, compensation

1. INTRODUCTION

Scientific research interest in β-Ga_2O_3 has seen a strong increase in the past decade. This has led to the development of high quality bulk single crystals,[1] the demonstration of unipolar devices[2] and the ability to effectively control *n*-type doping.[3] On the other hand, achieving p-type conductivity appears challenging – if not impossible – due to the large effective hole masses,[3] the self-trapping of holes,[4] and the tendency of acceptor states being deep rather than shallow.[5] The identification of dominating lattice defects is an important goal in order to further improve the properties of β-Ga_2O_3 devices.[1,6] In *n*-type doped semiconductors, the formation of acceptor-type native point defects is enhanced. These act as electrically compensating centers potentially limiting the conductivity through reduction of carrier concentration and increase in carrier scattering. Fortunately, the formation of native acceptors does not usually limit the carrier concentration except at very high doping levels.

The nature of the dominant native defect that forms and acts as a compensating center for a certain doping is a scientifically interesting question in itself. Technologically, it is important to understand whether the formation of this particular defect limits the desired functionality. In many materials, vacancy-type defects have the lower formation enthalpies and hence tend to be the dominant compensating defects. In *n*-type compound semiconductors, the cation (metal) vacancies are the typical dominant compensating native acceptor defects: V_{Ga} in GaN,[7] V_{Zn} in ZnO,[8] V_{In} in InN.[9] Notably in none of these materials is the compensation of *n*-type doping an issue. In β-Ga_2O_3, theoretical calculations[10] and early positron annihilation experiments[11] have suggested that V_{Ga} could be very efficient in the compensation of *n*-type conductivity, but systematic experimental evidence is lacking.

In more detail, theoretical calculations predict[10,12,13] that the energetically most favourable atomic configuration for the Ga vacancy is such that a Ga atom neighboring (next-nearest neighbor) the Ga mono-vacancy relaxes to an interstitial site half-way toward the original mono-vacancy. The open volume in this "split" Ga vacancy is divided on both sides of the interstitial, with an appearance of two "half-vacancies". Importantly, only one Ga atom is missing and hence this defect is by definition of mono-vacancy character. These split Ga vacancies were recently observed with scanning transmission electron microscopy.[14] In our recent work combining experiments and state-of-the-art modeling, we showed that split Ga vacancies have very distinct fingerprints in positron annihilation signals.[15] The anisotropy of these signals accounts for the directional dependence of the Doppler broadening noted in Ref. 16. In this contribution, we show that the split Ga vacancies dominate the positron annihilation characteristics of all β-Ga_2O_3samples studied so far, irrespective of their conductivity. The detailed understanding of the electrical compensation mechanisms in *n*-type β-Ga_2O_3 is still "under construction".

*filip.tuomisto@helsinki.fi; physics.helsinki.fi

Oxide-based Materials and Devices XII, edited by David J. Rogers, David C. Look
Ferechteh H. Teherani, Proc. of SPIE Vol. 11687, 1168709 · © 2021 SPIE
CCC code: 0277-786X/21/$21 · doi: 10.1117/12.2585462

2. METHOD

2.1 Material

The experimental positron annihilation data shown in this work are collected from samples discussed in detail in Refs. 11,15-17. The samples include homo-epitaxial thin films grown by metal-organic vapor phase epitaxy (MOVPE) and hydride vapor phase epitaxy (HVPE), as well as bulk crystals grown by the Czochralski (CZ) and edge-degined film-fed growth (EFG) methods. Samples with varying doping have been investigated: unintentionally doped (uid), Si-doped, Sn-doped, Mg-doped and Fe-doped. Generally, Si and Sn doping is used to achieve n-type conductivity while Mg and Fe doping for semi-insulating character.

2.2 Positron annihilation spectroscopy

Positron annihilation spectroscopy is a set of methods with particular use in the identification and quantification of negatively charged and neutral vacancy-type defects in semiconductors.[18] The concentration sensitivity range is 10^{15}–10^{19} cm^{-3}. By performing temperature-dependent experiments, the methods can distinguish between different charge states of the vacancies and give information on their chemical environment, in addition to the size of the open volume and the concentrations. In the experiments, relatively high energy positrons are implanted into the specimen where they stop, thermalize and diffuse and eventually annihilate with electrons emitting two 511-keV γ-quanta. Prior to annihilation, the positrons probe the interstitial space in a delocalized state in the crystal lattice and may get trapped at vacancy-type (open volume) defects thanks to the missing repulsive ion core. The trapping at vacancies causes changes in the commonly measured characteristics of the positron-electron annihilation radiation: the positron lifetime and the Doppler broadening of the 511 keV annihilation line. The former is inversely proportional to the overlap of the positron and electron densities and as most of the electrons are localized at the lattice atoms, the positron lifetime increases when the positron is trapped at a vacancy. In Doppler broadening, the momentum of the annihilating positron-electron pair causes a broadening of the 511 keV annihilation line due to energy and momentum conservation. For positrons trapped at vacancies, the probability of annihilation with high-momentum core electrons of the atoms is lower than for the free positrons in the delocalized state in the crystal lattice. Hence, usually positron trapping at vacancies is detected as a narrowing of the 511 keV line. Generally, the positron lifetime gives information about the open volume and concentration of the vacancy defects, while Doppler broadening gives information on the chemical surroundings of the vacancy, namely the electron configuration of the surrounding atoms.

In this work, we focus on the Doppler broadening results obtained in β-Ga_2O_3 samples, measured in either a fast-positron setup where a positron source (^{22}Na) is sandwiched between two identical pieces of sample material, or with a slow positron beam where positrons from a radioactive source are slowed down and implanted in a single sample at energies between 0–40 keV. Fast positrons probe the sample up to about 200 μm providing averaged data over these depths, while a slow positron beam is used to probe near-surface regions up to 2 μm below the surface. A slow positron beam is necessary for studying thin films. The energy resolution of the gamma detectors is usually relatively poor at high energies, and the broadening of the 511-keV annihilation peak is often characterized by the so-called *S* and *W* parameters. These are defined as the normalized areas (counts) of the center and wings of the peak, respectively. They are a measure of the fraction of positrons annihilating with low-momentum electrons (*S*) and high-momentum electrons (*W*). The *S* (*W*) parameter is a linear superposition of the characteristic *S* (*W*) parameters for annihilations in different positron states in the sample:

$$S(W) = \eta_b S_b\,(W_b) + \sum_i \eta_i S_i\,(W_i). \quad (1)$$

Here the subscript *b* refers to the free, delocalized Bloch state, in which the positron is in the defect-free crystal lattice. The weighting factors η are the fractions of positron annihilations at each state. The presence of vacancies therefore results in a higher *S* parameter and correspondingly a lower *W* parameter than in the defect-free lattice. If only one type of vacancy (*V*) traps positrons, (S,W) becomes a linear combination of the values (S_b,W_b) and (S_V,W_V), corresponding to the lattice and the vacancy, respectively. The measured values would thereby fall on a straight line connecting the points (S_b,W_b) and (S_V,W_V) on a *S*-*W* plot. The position on this line then reveals the concentration of these vacancies.

The Doppler broadening experiment is by definition direction-dependent: it is effectively a measurement of the the 3-dimensional momentum distribution $\rho(\mathbf{p})$ of the annihilating positron-electron pairs projected along the detection axis (L for longitudinal):

$$\rho(p_L) = \iint \rho(\mathbf{p}) dp_\perp. \quad (2)$$

Figure 1 shows typical measurement geometries in Doppler broadening experiments, performed with either fast or slow positrons. The "longitudinal" direction is typically along a crystal orientation within the sample surface, but in fast positron experiments it can be also along the surface normal. Typically, the sample surface is one with relatively high symmetry, such as (100) or (111), and also the sample edges are along high symmetry orientiations. When performing defect studies in 3D crystal structured "conventional" semiconductors (for example Si, GaAs, GaN, or ZnO) with positron annihilation, the measurement orientation is often disregarded, even if the Doppler broadening signals as defined by Eq. (2) are anistropic by nature as they are tightly connected to the crystal symmetries. This is warranted as the effect has been found to be negligible: The relative differences in the Doppler broadening signals in the different directions are of the order of 0.05 – 0.1% (S parameter) in these materials, while vacancy-type defects generate signal modification by 3 – 5 %.[15,19,20] The differences in the W parameter are 5-10-fold, but the relative importance of vacancies over the directional dependence is the same. Further, the anisotropy of the vacancy signals themselves has been observed to be less (at most similar) than the anisotropy of the signals originating from the "defect-free" lattice.[19]

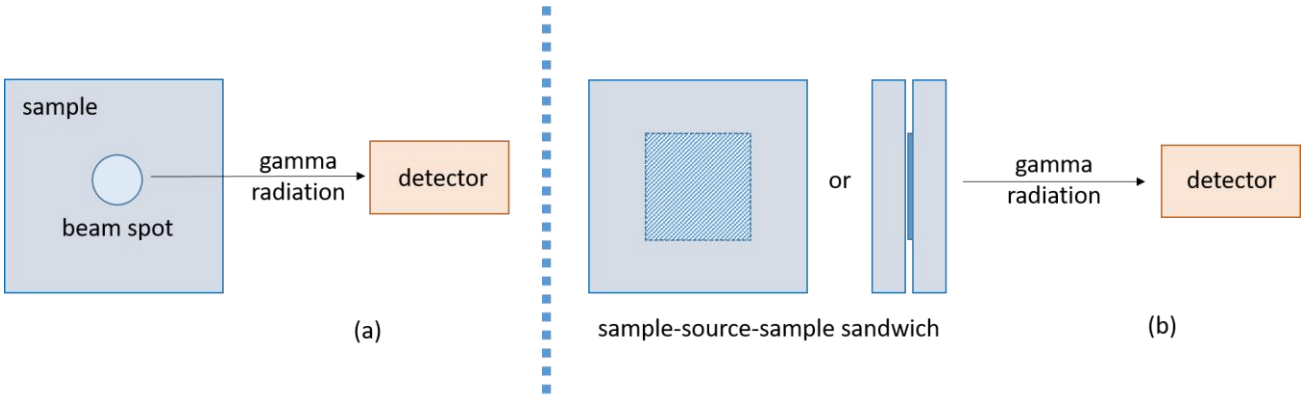

Figure 1. (a) Typical measurement geometry in a slow positron beam. The detector is aligned perpendicular to the incoming beam and hence to the surface normal, i.e., the direction of the measurement is along a crystal orientation within the surface plane of the sample. (b) Typical measurement geometry in a fast positron experiment. The detector is placed either in a similar orientation as in the slow positron beam experiment, or along the surface normal of the samples.

However, as pointed out in Ref. 16 and analyzed in detail in Ref. 19, β-Ga_2O_3 is colossally different from the above-mentioned semiconductors in terms of orientational dependence (anisotropy) of the Doppler broadening. In typical samples measured with a slow positron beam, a rotation of the sample by 90 degrees leads to relative change of the S parameter by 2 – 4%, almost two orders of magnitude more than in, e.g., ZnO and of similar magnitude as typical vacancy effects.[15,20] This magnitude of anisotropy has earlier been observed or theorized only in systems with fundamentally lower symmetry, such as graphite or carbon nanotubes.[21,22] State-of-the-art theoretical calculations predict that the positron state in the β-Ga_2O_3 lattice is fundamentally of 1-dimensional tubular nature, as opposed to the positron state that forms 3-dimensional networks in the more symmetric diamond, zincblende or wurtzite lattices of Si, GaAs or GaN.[15] However, the detailed mechanisms giving rise to the colossal anisotropy of the Doppler broadening signals in β-Ga_2O_3 are still to be elucidated. Nevertheless, in positron annihilation studies in β-Ga_2O_3 it is of utmost importance to pay close attention to the measurement direction and give a detailed account of the measurement geometry.

In this work, we present experimental (S, W) data obtained with high-purity Ge (HPGe) detectors with either 1.15 keV or 1.25 keV (full width at half maximum, FWHM) energy resolution at 511 keV, depending on the employed setup. $1 - 3 \times 10^6$ counts were collected in each spectrum. The *S* and *W* parameter integration windows were set as 0 – 0.45 a.u. and 1.5 – 4.1 a.u., respectively. In order to perform measurements in multiple crystal orientations, a special sample holder was used allowing for full 3D rotation in the fast positron experiments (Fig. 1b). In beam experiments, sample rotation is much less practical and restricted to rotation around the sample surface normal – here typically only two perpendicular directions are measured (Fig. 1a). We also present results obtained with state-of-the-art *ab initio* theoretical calculations of the positron annihilation signals. For details on the experimental and theoretical approaches, see Refs. 15 and 18.

3. RESULTS

3.1 Theoretical calculations

Figure 2 shows the calculated (S, W) parameters for the β-Ga_2O_3 lattice and selected vacancy-type defects determined along the three highest-symmetry crystal orientations [100], [010] and [001], where the non-orthogonal 103.7° angle is between [100] and [001]. The examples a selected to best represent the different anisotropic behavior found in the various types of defects.[15,17] It is worth noting that the [010] direction produces systematically the highest *S* (and lowest *W*) parameters. Note also that the calculations allow to determine the (S, W) parameters along arbitrary directions but for simplicity we show only those with the highest-symmetry. In most cases these are also extrema in the (*S*, *W*) plot. For detailed analysis of the behavior of the (*S*, *W*) parameters in full 3D, see Ref. 15. The (S, W) parameters shown in Fig. 2 are normalized to those calculated for the [001] direction, following the convention adopted in Ref. 15. This allows for straightforward analysis of the relative changes caused by the anisotropy.

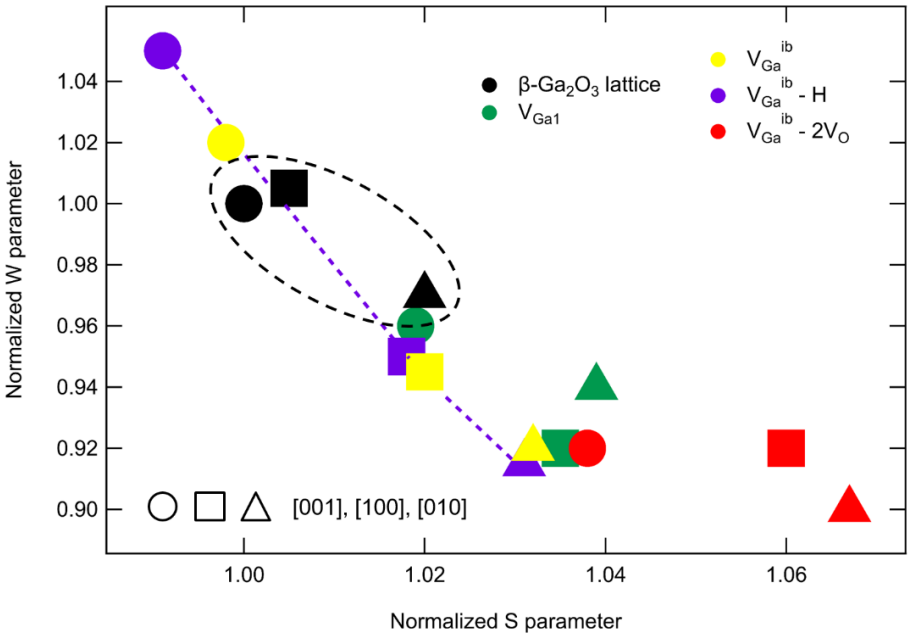

Figure 2. Calculated (S, W) parameters for the β-Ga_2O_3 lattice and selected vacancy-type defects in the three highest-symmetry directions [001], [010] and [100]. The parameters are shown as normalized to the β-Ga_2O_3 lattice in the [001] direction, following the convention in Ref. 15. The parameters of the lattice are surrounded with a dashed oval to guide the eye, and the largest anisotropy exhibited by the V_{Ga}^{ib}-H defect is highlighted with a dashed line.

The calculated data shown in Fig. 2 highlight all the peculiarities of positron data encountered in β-Ga_2O_3. The most striking feature is the colossal anisotropy of the (*S*, *W*) parameters observed along the different lattice directions. Note that the anisotropy in, e.g., Si or ZnO is smaller than the marker size in Fig. 2.[15] The unrelaxed Ga vacancy exhibits similarly

large anisotropy as the β-Ga_2O_3 lattice, exemplified by the data in V_{Ga1} (the Ga vacancy with 4 nearest-neighbor O atoms). The split Ga vacancies are represented by V_{Ga}^{ib} and its complexes with H and 2 O vacancies. Note that there are three different types of split Ga vacancies (ia, ib and ic), whose identity depends on the participation of the two inequivalent Ga sites in the defect.10,15 V_{Ga}^{ib} and V_{Ga}^{ib} –H demonstrate the most striking feature of the positron data in β-Ga_2O_3. The (*S*, *W*) parameters of the split Ga vacancies completely overlap with the lattice data, and in addition exhibit anisotropy that is significantly larger than that exhibited by the lattice or by any other defects considered so far, including larger vacancy complexes. Only Ga vacancies complexed with multiple O vacancies, exemplified in Fig. 2 by V_{Ga}^{ib} –$2V_O$ generate clearly separate data irrespective of the measurement orientiation.[17]

3.2 Experimental data

Figure 3 shows measured (S, W) parameters in a wide variety of β-Ga_2O_3 samples with the slow positron beam and fast positron setups, in high-symmetry crystal orientations. The data have been adjusted for the different detector resolutions and measurement geometries (by measuring some of the crystals with both setups) so that they can be shown in the same figure. Note that as the exact origin of the positron annihilation signals in β-Ga_2O_3 samples has not yet been established, the data cannot be normalized to a well-defined reference point as in the case of the theoretical calculations or materials where a "defect-free" reference sample has been characterized in detail. Hence we present the "raw" *S* and *W* parameters in Fig. 3. The data are shown for a Mg-doped (semi-insulating) CZ crystal, Fe-doped (semi-insulating), Sn-doped (n-type) and undoped (n-type) EFG crystals, and a Si-doped (n-type) thin film.[15-17]

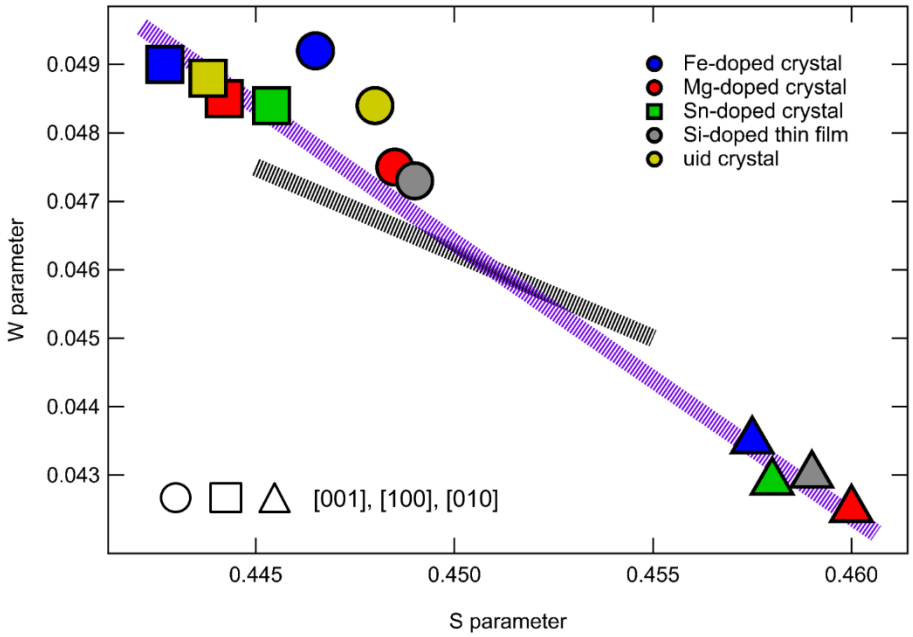

Figure 3. Experimentally determined (S, W) parameters for various β-Ga_2O_3 samples. The data have been adjusted for the differences in the energy resolutions and measurement geometries in different setups. The marker size corresponds to the experimental error bar. The purple and black shadowed scale bars represent the overall anisotropy of the V_{Ga}^{ib}-H and the β-Ga_2O_3 lattice shown in Fig. 2, respectively.

The first observation to be made from Fig. 3 is that the [010] direction gives the highest *S* (and lowest *W*) parameters, similar to the tendency in the calculated data. The second, more important observation is that the overall magnitude of the anisotropy in the experimental (S, W) parameters is colossal for all samples, comparable in magnitude only to the largest anisotropy found in the calculations for the split Ga vacancies. Figure 3 shows the overall magnitude of the anisotropy for the V_{Ga}^{ib}-H and the β-Ga_2O_3 lattice for comparison. Even in the undoped (uid) crystal, where only [001] and [100] could be easily measured as there was only one piece of sample available, it is clear that the difference between these two

orientations is much larger than that predicted for the β-Ga_2O_3 lattice (see Fig. 2). Note that all the samples exhibit very similar behavior irrespective of the doping or type of conductivity.

4. DISCUSSION

Comparing the experimental (Fig. 3) and theoretically calculated (Fig. 2) Doppler broadening data leads to a simple conclusion: the positron data in are dominated by split Ga vacancies in all the β-Ga_2O_3 samples, irrespective of type of dopant or conductivity. The dominance of the split Ga vacancy signal indicates that their concentrations are at the level of 10^{18} cm^{-3} or higher. This is remarkable as the doping concentrations in the n-type samples are of the same order of magnitude,[16,17] suggesting that the electrical compensation caused by these split Ga vacancies is not necessarily very efficient. Interestingly, the original data in Ref. 10 suggest that in the semi-insulating samples where high Ga vacancy concentrations were detected, the vacancies have much larger open volume than the split vacancies, such as found in unrelaxed Ga vacancies or (split) Ga vacancy – O vacancy complexes.[17] Very recent experiments in H implanted β-Ga_2O_3 suggest[23] that the interplay between H and the various types of Ga vacancies is the key to understanding the electrical compensation in n-type β-Ga_2O_3, and further work is still required to elucidate the mechanisms.

Closer inspection of Figs. 2 and 3 reveals that the detailed identities of the split Ga vacancies in the β-Ga_2O_3 samples cannot yet be revealed. While the overall magnitude of the anisotropy in the experiments generally corresponds to that of the split Ga vacancies (also ic type[15]), the detailed behavior in particular in the [001] and [100] directions is different in experiments and theory. Note, however, that the overall anisotropy in experiments should be smaller than in theoretical calculations due to the finite aspect ratio of the detector geometry.[15] The detailed identification is also complicated by the fact that temperature-dependent positron lifetime experiments discussed in detail in Ref. 17 show that most of the crystals contain a distribution of several types of defects, all contributing to the Doppler broadening signals. Further work is still required for full identification of the (split) Ga vacancy defects that are clearly abundant in β-Ga_2O_3.

5. SUMMARY

We have performed positron annihilation spectroscopy in Doppler broadening mode on a wide range of β-Ga_2O_3 bulk crystals and thin films with various doping levels. We compare the results to state-of-the-art theoretical calculations. The Doppler broadening signals, characterized by the *S* and *W* parameters, exhibit colossal anisotropy earlier found only in fundamentally low-dimensional systems such as graphite or carbon nanotubes. Utilizing this anisotropy for defect identification allows us to conclude that almost all β-Ga_2O_3 samples studied so far contain significant, at least 10^{18} cm^{-3}, concentration of split Ga vacancies. As this finding holds irrespective of doping or conductivity, the electrical compensation of n-type β-Ga_2O_3 is more complicated than simple formation of acceptor-type vacancy defects. Further work is in progress to elucidate the detailed mechanisms governing the formation of compensating defects in *n*-type β-Ga_2O_3.

REFERENCES

[1] Pearton, S. J., Yang, J., Cary IV, P. H., Ren, F., Kim, J., Tadjer, M. J., and Mastro, M. A., "A review of Ga_2O_3 materials, processing, and devices", Appl. Phys. Rev. 5, 011301 (2018).

[2] Higashiwaki, M., Murakami, H., Kumagai, Y., and Kuramata, A., "Current status of Ga_2O_3 power devices", Jpn. J. Appl. Phys. 55, 1202A1 (2016).

[3] Zhang, J., Shi, J., Qi, D.-C., Chen, L., and Zhang, K. H. L., "Recent progress on the electronic structure, defect, and doping properties of Ga_2O_3", APL Materials 8, 020906 (2020).

[4] Varley, J. B., Janotti, A., Franchini, C., and Van de Walle, C. G., "Role of self-trapping in luminescence and p-type conductivity of wide-band-gap oxides", Phys. Rev. B 85, 081109 (2012).

[5] Kyrtsos, A., Matsubara, M., and Bellotti, E., "On the feasibility of p-type Ga_2O_3", Appl. Phys. Lett. 112, 032108 (2018)

[6] McCluskey, M. D., "Point defects in Ga_2O_3", J. Appl. Phys. 127, 101101 (2020).

[7] Tuomisto, F., Ranki, V., Look, D. C., and Farlow, G. C., "Introduction and recovery of Ga and N sublattice defects in electron-irradiated GaN", Phys. Rev. B 76, 165207 (2007).
[8] Tuomisto, F., Ranki, V., Saarinen, K., and Look, D.C., "Evidence of the Zn Vacancy Acting as the Dominant Acceptor in n-Type ZnO", Phys. Rev. Lett. 91, 205502 (2003).
[9] Reurings, F., Tuomisto, F., Gallinat, C. S., Koblmüller, G., and Speck, J. S., "In vacancies in InN grown by plasma-assisted molecular beam epitaxy", Appl. Phys. Lett. 97, 251907 (2010).
[10] Varley, J. B., Peelaers, H., Janotti, A., and Van de Walle, C. G., "Hydrogenated cation vacancies in semiconducting oxides", J. Phys.: Condens. Matter 23, 334212 (2011).
[11] Korhonen, E., Tuomisto, F., Gogova, D., Wagner, G., Baldini, M., Galazka, Z., Schewski, R., and Albrecht, M., "Electrical compensation by Ga vacancies in Ga2O3 thin films", Appl. Phys. Lett. 106, 242103 (2015).
[12] Lany, S., "Defect phase diagram for doping of Ga_2O_3", APL Mater. 6, 046103 (2018).
[13] Ingebrigtsen, M., Kuznetsov, A. Yu., Svensson, B. G., Alfieri, G., Mihaila, A., Badstübner, U., Perron, A., Vines, L., and Varley, J. B., "Impact of proton irradiation on conductivity and deep level defects in β-Ga_2O_3", APL Mater. 7, 022510 (2019).
[14] Johnson, J. M., Chen, Z., Varley, J. B., Jackson, C. M., Farzana, E., Zhang, Z., Arehart, A. R., Huang, H.-L., Genc, A., Ringel, S. A., Van de Walle, C. G., Muller, D. A., and Hwang, J., "Unusual Formation of Point-Defect Complexes in the Ultrawide-Band-Gap Semiconductor β-Ga_2O_3", Phys. Rev. X 9, 041027 (2019).
[15] Karjalainen, A., Prozheeva, V., Simula, K., Makkonen, I., Callewaert, V., Varley, J. B., and Tuomisto, F., "Split Ga vacancies and the unusually strong anisotropy of positron annihilation spectra in β-Ga_2O_3", Phys. Rev. B 102, 195207 (2020).
[16] Tuomisto, F., Karjalainen, A., Prozheeva, V., Makkonen, I., Wagner, G., and Baldini, M. "Ga vacancies and electrical compensation in β-Ga_2O_3 thin films studied with positron annihilation spectroscopy", Proc. SPIE 10919, Oxide-based Materials and Devices X, 1091910 (1 March 2019).
[17] Karjalainen, A., Makkonen, I., Etula, J., Goto, K., Murakami, H., Kumagai, Y., and Tuomisto, F., "Split Ga vacancies in n-type and semi-insulating β-Ga_2O_3 single crystals", Appl. Phys. Lett., in press.
[18] Tuomisto, F. and Makkonen, "Defect identification in semiconductors with positron annihilation: Experiment and theory", Rev. Mod. Phys. 85, 1538 (2013).
[19] Dannefaer, S., Puff, W., and Kerr, D., "Positron line-shape parameters and lifetimes for semiconductors: Systematics and temperature effects", Phys. Rev. B 55, 2182 (1997).
[20] Zubiaga, A., Tuomisto, F., Zuñiga-Pérez, J., and Muñoz-San José, V., "Characterization of non-polar ZnO layers with positron annihilation spectroscopy", Acta Phys. Pol. A 114, 1457 (2008).
[21] Kanazawa, I., Tanigawa, S., Suzuki, R., Mizuhara, Y., Sano, M., and Inokuchi, H., "Two-dimensional electron momentum distribution in graphite revealed by means of angular correlation of positron annihilation", J. Phys. Chem. Solids 48, 701 (1987).
[22] Ishibashi, S., "Calculation of positron states in carbon-nanotube bundles", J. Phys.: Condens. Matter 14, 9753 (2002).
[23] Karjalainen, A., Weiser, P. M., Makkonen, I., Reinertsen, V., Vines, L., and Tuomisto, F., "Interplay of vacancies, hydrogen, and electrical compensation in irradiated and annealed *n*-type β-Ga_2O_3", submitted to J. Appl. Phys.